Bifurcation analysis of a menstrual cycle model reveals multiple mechanisms linking testosterone and classical PCOS ☆

Q1 Angelean O. Hendrix [a,1,2], James F. Selgrade [a,b,*]

[a] Department of Mathematics, North Carolina State University, Raleigh, NC 27695-8205, United States
[b] Biomathematics Program, North Carolina State University, Raleigh, NC 27695, United States

HIGHLIGHTS

- Deterministic model for hormonal regulation of the menstrual cycle includes testosterone.
- Various characteristics of polycystic ovarian syndrome are illustrated.
- Model simulations reveal anovulatory and hyperandrogenic cycles menstrual cycles.
- Bifurcations with respect to sensitive parameters are studied.

ARTICLE INFO

ABSTRACT

A system of 16 differential equations is described which models hormonal regulation of the menstrual cycle focusing on the effects of the androgen testosterone (T) on follicular development and on the synthesis of luteinizing hormone (LH) in the pituitary. Model simulations indicate two stable menstrual cycles – one cycle fitting data in the literature for normal women and the other cycle being anovulatory because of no LH surge. Bifurcations with respect to sensitive model parameters illustrate various characteristics of polycystic ovarian syndrome (PCOS), a leading cause of female infertility. For example, varying one parameter retards the growth of preantral follicles and produces a "stockpiling" of these small follicles as observed in the literature for some PCOS women. Modifying another parameter increases the stimulatory effect of T on LH synthesis resulting in reduced follicular development and anovulation. In addition, the model illustrates how anovulatory and hyperandrogenic cycles which are characteristic of PCOS can be reproduced by perturbing both pituitary sensitivity to T and the follicular production of T. Thus, this model suggests that for some women androgenic activity at the levels of both the pituitary and the ovaries may contribute to the etiology of PCOS.

© 2014 Published by Elsevier Ltd.

1. Introduction

The control and maintenance of the human menstrual cycle involves hormones produced by the brain and ovaries. Follicle stimulating hormone (FSH) and luteinizing hormone (LH), which are secreted via actions of the hypothalamus and the pituitary glands, regulate ovarian hormone synthesis and the periodic release of an ovum, e.g., see Hotchkiss and Knobil (1994), Yen (1999a), and Zeleznik et al. (1994). In turn, the ovaries produce estradiol (E2), progesterone (P4), inhibin A (InhA), inhibin B (InhB) and testosterone (T) which influence the synthesis and release of FSH and LH, e.g., see Karch et al. (1973), Liu and Yen (1983), and Wang et al. (1976). The menstrual cycle is evenly divided into two phases, the follicular phase and the luteal phase, separated by ovulation (Ojeda, 2012; Yen, 1999b; Gougeon, 1986). The cycle begins with the first day of menstrual flow. At that time, blood levels of FSH rise to promote the recruitment and growth of immature follicles. Midway through the follicular phase, typically the growth of one dominant follicle surpasses the rest which then begin to atrophy. This dominant follicle grows rapidly and produces E2 in large amounts. E2 primes the pituitary for LH synthesis. E2 peaks and one day later LH peaks at 8 to 10 times its early follicular concentration. This rapid rise and fall of LH over a period of 5 days is referred to as the LH surge and is necessary for

ovulation. The LH surge followed by ovulation transforms the dominant follicle into the corpus luteum. The corpus luteum is responsible for increased secretion of E2, P4, and the inhibins which prepare the uterus for pregnancy and which suppress the production of FSH and LH. If fertilization and implantation do not occur then the corpus luteum decreases in size and hormone secretion and becomes inactive by the end of the menstrual cycle. The consequential rise in FSH initiates the next cycle.

Many cycle irregularities are associated with abnormal levels of some of these hormones. In particular, polycystic ovarian syndrome (PCOS) is the leading cause of female infertility in North America and afflicts 6–9% of all adult women (Alvarez-Blasco et al., 2006; Azziz et al., 2004; Yen, 1999b; Franks et al., 2008). PCOS is characterized by irregular follicle development which usually results in anovulation. PCOS women often exhibit high androgen levels, low P4, acyclic E2, and an increased ratio of LH to FSH. Understanding how variations in hormone levels and key ovarian growth parameters alter follicular development may predict ovulatory difficulties and may suggest therapies for PCOS.

Mathematical models for hormonal control of the menstrual cycle may be useful for addressing these issues. Systems of differential equations have been developed to describe mechanistic models of cycle regulation which capture the complex signaling between the brain and the ovaries. Examples of models with this approach include Bogumil et al. (1972, 1972), Plouffe and Luxenberg (1992), Harris-Clark et al. (2003), Zeeman et al. (2003), Reinecke and Deuflhard (2007), Pasteur (2008), Röblitz et al. (2013), Margolskee and Selgrade (2013), and Chen and Ward (2014).

Building on these models, Hendrix (2013) and Hendrix et al. (2014) have introduced a system of 16 differential equations (Eqs. (S1–S16) and (A1–A5) in Appendix A) to model the effects of testosterone, a prominent ovarian androgen for which serum data exist in the literature, on follicular development and on gonadotropin releasing hormone receptor priming in the pituitary. The data for LH, FSH, E2, P4, InhA, and InhB from Welt et al. (1999) and for total T from Sinha-Hikim et al. (1998) were used to optimized parameters.

The new model contains stages of ovarian development which represent preantral and early antral follicles and simulations exhibit an attracting periodic solution (Hendrix et al., 2014) which approximates well the hormone levels of a normally cycling woman (Welt et al., 1999; Sinha-Hikim et al., 1998). Maciel et al. (2004) reported a "stockpiling" of preantral follicles in women with PCOS. Hendrix et al. (2014) illustrated how varying a single parameter which prolonged the growth of the preantral follicular stage resulted in irregular menstrual cycles similar to PCOS. In fact, additional changes in this parameter produced a period-doubling cascade of bifurcations resulting in chaotic menstrual cycle behavior.

In Hendrix et al. (2014), this dynamical behavior was discovered from numerical experimentation not bifurcation analyses. Moreover, many of the PCOS cycles presented in Hendrix et al. (2014) are anovulatory but do not exhibit elevated levels of androgens in the blood, which is common with PCOS patients. In order to understand more fully how the model introduced in Hendrix et al. (2014) predicts PCOS phenotypes, in this study we investigate in more depth the dynamical behavior of the model focusing on the roles of testosterone at the levels of the brain and the ovaries. We examine the stability and instability of periodic solutions. After setting the time-delays to zero and reparameterizing, we employ the bifurcation software XPPAUT (Ermentrout, 2002) which is designed for autonomous ordinary differential equations (not delay differential equations). We analyze bifurcations resulting from variations in sensitive parameters and we determine the existence and significance of hysteresis curves in

bifurcation diagrams. For example, we show that changing one parameter can increase the stimulatory effect of T on LH synthesis and simultaneously reduce the inhibitory effect of P4 on LH synthesis. Higher basal levels of LH and a normal LH surge are achieved, but follicular development is reduced to such an extent that no ovulation occurs. Hence, increased pituitary sensitivity to androgens as a cause of anovulation is demonstrated by our model behavior. Furthermore, we show that anovulatory and hyperandrogenic cycles can be reproduced by perturbing both the pituitary sensitivity to T and the follicular production of T. Thus, this model suggests that for some women androgenic activity at the levels of both the pituitary and the ovaries may contribute to the etiology of PCOS.

Section 2 describes some biological background and the model structure. Section 3 argues that it is reasonable to set the time-delays to zero so XPPAUT may be used, discusses parameter identification, and illustrates the bistable behavior. The bifurcation diagram with respect to the "stockpiling" parameter (m_2 in Eq. (S5)) is explained in Section 4. Section 5 draws the bifurcation diagram with respect to the pituitary sensitivity parameter (κ in Eq. (S1)) and discusses dynamical behavior for various ranges of κ values. Section 6 shows κ bifurcation diagrams for increased follicular production of T and illustrates anovulatory hyperandrogenic cycles.

2. Model background and development

2.1. Androgenic pituitary feedback

Gonadatrophin releasing hormone (GnRH) produced by the hypothalamus stimulates pituitary gonadotroph synthesis of LH at higher GnRH frequencies and FSH at lower frequencies (Blank et al., 2006). Original modeling efforts by Schlosser and Selgrade (2000) combined the actions of the hypothalamus and the pituitary in a system of four differential equations for the synthesis, release, and clearance of the gonadotrophin hormones. State variables RP_{LH} and RP_{FSH} represent the amounts of synthesized hormones in the pituitary; LH and FSH represent the blood concentrations of these hormones (see Eqs. (S1–S4) in Appendix A). Schlosser and Selgrade (2000) assume that E2 inhibits the release of the gonadotrophin hormones (see the denominators in the second terms of (S1) and (S3)) but at high levels E2 significantly promotes LH synthesis (see the Hill function in the numerator of the first term of (S1)). Progesterone and inhibin inhibit LH and FSH synthesis, in the respective denominators. Blood clearance rates for the gonadotropin hormones are taken proportional to their concentrations. Discrete time-delays are assumed for the effects of E2, P4 and inhibin on gonadotropin synthesis because hormone synthesis may not be as immediate as hormone release.

Recently much attention has been focused on investigations of androgen feedback on the pituitary as elevated levels significantly correlate with reproductive cycle disruption found in patients with polycystic ovarian syndrome (PCOS) (Azziz et al., 2009). Immuno-histochemical staining has localized androgen receptors (AR) in rat and human female anterior pituitary sections in concentrations similar to those in males (Sar et al., 1990; Takeda et al., 1990) suggesting a direct role of androgens in controlling LH secretion. According to studies (Yasin et al., 1996), androgens may prime gonadotrophs for GnRH activation through facilitation of LHβ mRNA expression. Female androgens, T and dihydrotestosterone (DHT), have both been found to affect positively gonadotroph synthesis of LH. As only T is a precursor to E2, this suggests the androgenic action at the pituitary level is independent of the conversion of T to E2 (Yasin et al., 1996). In rats, pituitary feedback

has also been shown to occur through androgen increased GABAergic transmission to GnRH neurons (Pielecka et al., 2006). In addition, isolated rat GnRH neurons have been shown to display increase pulse frequency in the presence of T and that would suggest an increased LH synthesis response (Melrose and Gross, 1987). The role of the androgens is further supported in clinical studies of flutamide treatment in PCOS patients. Flutamide, an androgen receptor blocker, has shown promising results in restoring cyclicity in anovulatory patients during long term clinical trials (Eagleson et al., 2000; De Leo and Morgante, 1998).

Motivated by these studies, Hendrix et al. (2014) assumed that the baseline LH synthesis rate is independent of E2 but depends on T, as expressed in the first term of the numerator of Eq. (S1). Testosterone is used to represent ovarian androgen feedback as it is currently considered the most potent of the female androgens for which levels are available in the literature across the menstrual cycle (Sinha-Hikim et al., 1998). We also note that in many investigations of hyperandrogenic menstrual disruption, Total T is often used as indicative of overall androgen levels (Sinha-Hikim et al., 1998). As current research has yet to suggest a similar role for the production of FSH, in Appendix A we present the system (S1–S4) of four equations for LH and FSH synthesis and release with further details available in Schlosser and Selgrade (2000) and Hendrix et al. (2014).

2.2. Intra-ovarian androgenic stimulation of early folliculogenesis

Pituitary production of FSH during the follicular phase of the cycle stimulates rapid growth of 6–12 follicles. These larger antral follicles produce T which stimulates the growth of smaller preantral follicles and which is partially converted to E2 because of FSH stimulation. During the follicular phase, a dominant follicle is chosen and produces E2 in large amounts eliciting the LH surge. After releasing its ovum, the dominant follicle is transformed into the corpus luteum (CL), which produces P4 to inhibit LH synthesis and InhA to inhibit FSH synthesis. Also, P4 prepares the endometrium for implantation in the event of fertilization. If a viable zygote is not detected then the CL slowly atrophies, removing the negative feedback of P4 and InhA and allowing a new wave of FSH stimulated follicular growth. These events signal the transition from luteal to follicular phase and mark the beginning of a new menstrual cycle.

Using the model structure of Harris-Clark et al. (2003), Hendrix et al. (2014) introduced 12 differential equations (S5–S16) in Appendix A where each state variable represents the hormonally active mass of a distinct stage of ovarian development. Transition from one stage to the next is promoted by the gonadotropin hormones and/or intra-ovarian growth factors, including T. In order of development, the 12 stages are two preantral follicular stages (*PrA* 1 and *PrA* 2), small antral follicles (*SmAn*), recruited follicles (*RcF*), the dominant follicle (*DmF*), the ovulatory follicle (*OvF*), two stages portraying the transition to the corpus luteum (*CL* 1 and *CL* 2) and four luteal stages *Lut*i, $i = 1, \ldots, 4$. The first three stages consist of small follicles growing as much as 60 days before they would ovulate. For these stages, mass action kinetics reflect intra-ovarian signaling (S5–S7) with T dependent growth occurring before FSH stimulated growth (S5–S6). The monthly cycling stages, *RcF* through *Lut* 4, depend on the gonadotropin hormones. Clearance from the blood of the ovarian hormones is on a fast time scale (Baird et al., 1969) as compared to ovarian development and to clearance of the pituitary hormones, so the ovarian hormones are assumed at a quasi-steady state (Keener and Sneyd, 2009). Thus, the auxiliary equations (A1–A5) give the serum concentrations of the five ovarian hormones. Preantral and small antral follicles produce InhB and T, so *PrA* 2 and *SmAn* terms are included in (A4) and (A5). See Hendrix et al. (2014) for details.

3. Parameter identification, sensitivities and bistability

Using discrete log difference approximations, Hendrix (2013) computed normalized sensitivity coefficients for the system (S1–S16). A normalized sensitivity coefficient estimates the amount of variation in a system output with respect to small variation in a system parameter by approximating a partial derivative of the output variable with respect to the parameter, normalized so that comparisons may be made among variables and parameters. In Hendrix et al. (2014), the only nonzero time-delay parameters were of duration 1 day for the inhibitions of P4, InhA, and InhB in (S1) and (S3). The normalized sensitivity coefficients for these delay parameters, d_P, d_{InhA} and d_{InhA}, were at most 0.1 and quite small when compared with sensitivities of 1 or larger (Hendrix, 2013). Thus, for this study, we set the time-delays equal to zero and refit system parameters to the data of Welt et al. (1999) and of Sinha-Hikim et al. (1998) to obtain the optimized values in Tables B1–B3. The parameters of Appendix B are obtained by using a Nelder-Mead simplex method (Nelder and Mead, 1965; Wright, 1996) starting with the parameters of Hendrix et al. (2014). Henceforth, we study equations (S1–S16) with the parameters of Tables B1–B3 where the time-delays are zero.

Simulations for this model exhibit two locally asymptotically stable periodic solutions (see Fig. 1 for E2 and LH). One solution (the dashed curves in Fig. 1) approximates well the data of Welt et al. (1999), has a period of 27 days, and represents a menstrual cycle for which ovulation occurs because of adequate E2 and a normal LH surge. The other periodic solution (the solid curves in Fig. 1) has a period of approximately 23 days and represents an anovulatory cycle because there is no LH surge. We refer to these solutions as the normal and the abnormal cycle, respectively. Notice that E2 levels for the abnormal cycle vary slightly over the month and remain below 140 pg/mL. On the other hand, E2
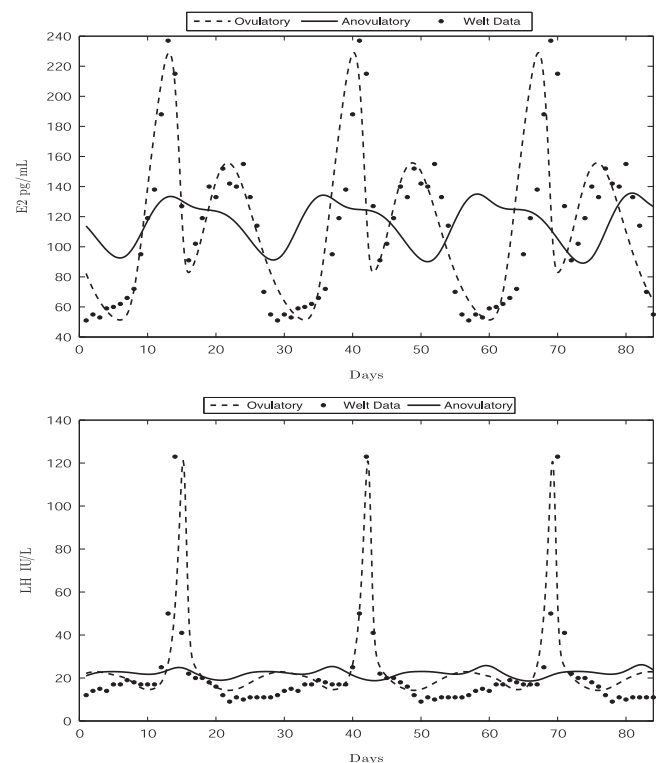

Fig. 1. E2 and LH model simulations for (S1–S16) with parameters and initial conditions given in Appendix B. 28 day data from Welt et al. (1999) are repeated for 84 days. The dashed curves depict normal cycles and the solid curves, abnormal cycles.

during the follicular phase of the normal cycle exceeds 220 pg/mL and, thus, elicits an LH surge. For the abnormal cycle, FSH and P4 concentrations are similarly lower than those of the normal cycle. These characteristics are present in many PCOS individuals, see Yen (1999a) and Azziz et al. (2009).

Bistability of the type illustrated by Fig. 1 has been observed for similar hormone control models by Harris-Clark et al. (2003) and Selgrade et al. (2009). As demonstrated in Harris-Clark et al. (2003), the abnormal cycle may be perturbed to the normal cycle by the administration of exogenous P4 during the luteal phase and the normal cycle may be perturbed to the abnormal by exogenous E2. Moreover, small variations in sensitive parameters may result in bifurcations which remove the abnormal cycle and produce a model with a unique asymptotically stable solution and this solution represents an ovulatory menstrual cycle (see Section 4).

4. Bifurcation analysis for parameter m_2

Hendrix et al. (2014) showed how varying the sensitive parameter m_2 (see Eq. (S5)) produced significant changes in model behavior. Decreasing m_2 permits additional growth of preantral follicles PrA 1 and results in a "stockpiling" of these small follicles as observed by Maciel et al. (2004) in PCOS women. In fact, Hendrix et al. (2014) illustrates a period-doubling cascade of bifurcations as m_2 decreases, resulting in apparent chaotic menstrual cycle behavior. Here we examine the bifurcation diagram with respect to m_2 using the software XPPAUT (Ermentrout, 2002), which is appropriate for systems without time-delays. Because the optimal value $m_2 = 0.000868$ (see Table B2) is so small and very small variations result in bifurcations, to illustrate these bifurcations it is useful to apply XPPAUT to the parameter $l_2 = \log(m_2)$, where log is the natural logarithm. (Taking log of a set of numbers close to zero spreads the set out.)

For each value of the parameter l_2 on the horizontal axis (Fig. 2), the software XPPAUT plots a state variable value for each stable periodic (or equilibrium) solution and each unstable periodic solution of the dynamical system which it finds at that parameter value. Since the height of the LH surge is a good indicator of an ovulatory cycle, we take LH as our state variable
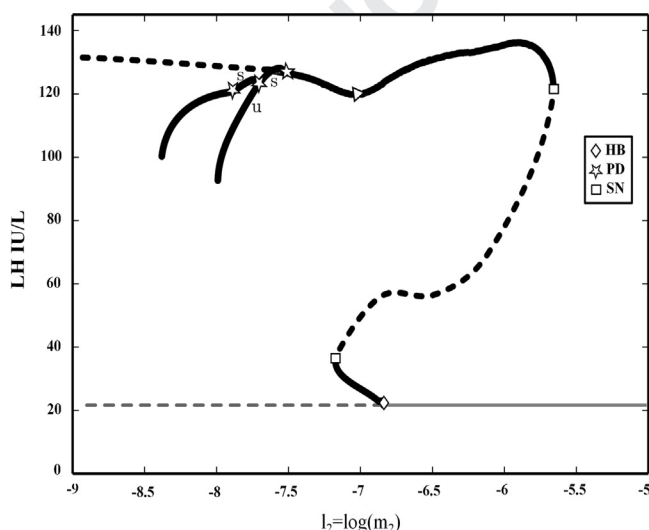

Fig. 2. Bifurcation diagram with respect to $l_2 = \log(m_2)$ for (S1–S16) with remaining parameters from Tables B1–B3. HB, SN and PD denote Hopf, saddle-node and period-doubling bifurcations. The △ indicates the position ($l_2 = -7.05$) of the normal cycle for the parameters of Tables B1–B3. Heavy solid (dashed) curves denote stable (unstable) cycles. Light solid (dashed) curves denote stable (unstable) equilibria. To the left of the second PD bifurcation all periodic solutions are solid curves, so s denotes stable cycles and u denotes unstable cycles.

and our bifurcation diagram (Fig. 2) plots the maximum LH value along a periodic or equilibrium solution. As l_2 varies, curves evolve which represent the continuations of stable and unstable solutions. Generally, bifurcations occur where curves of differing stabilities meet.

For values of l_2 larger than -5.66, the only stable solution is an equilibrium (the solid line in the lower right of Fig. 2), which represents an anovulatory cycle because the LH level is too low. A saddle-node bifurcation (upper SN) of periodic solutions occurs at $l_2 = -5.66$ resulting in stable cycles (upper solid curve) and unstable cycles (lower dashed curve) as l_2 decreases. The stable cycle is ovulatory and continues to the normal cycle (△ in Fig. 2) corresponding to the model's optimal parameter value, $l_2 = -7.05 = \log(0.000868)$. At $l_2 = -6.81$, the stable equilibrium undergoes a Hopf bifurcation (HB) which results in a stable periodic solution (solid curve) and an unstable equilibrium (the dashed line that continues to the left from HB). This stable anovulatory cycle exists until $l_2 = -7.17$ where it coalesces with the unstable cycle and both disappear via a saddle-node (lower SN). For l_2 between -7.54 and -7.17, the only stable solution is the ovulatory cycle along the upper portion of the figure. At $l_2 = -7.54$, a period-doubling bifurcation (PD) causes the stable ovulatory cycle to become unstable and a stable solution of twice the period to appear (solid curve branching off below first PD). This stable solution represents two monthly ovulatory cycles. More period-doublings occur as l_2 decreases through -7.72 and through -7.74. The software has difficulty tracking rapidly occurring PD bifurcations, so only 3 are depicted in Fig. 2. The solid curves emanating from the PD's indicate stable (labeled s) or unstable (labeled u) periodic solutions. The PD at $l_2 = -7.72$ indicates a bifurcation of cycles with twice the original period to cycles with four times the original period. The PD at $l_2 = -7.74$ indicates a bifurcation of cycles with four times the period to eight times the period. This period-doubling cascade is discussed by Hendrix et al. (2014).

The sigmoid shaped curve in the right half of Fig. 2, which contains stable and unstable cycles, is referred to as a hysteresis curve or loop. For each l_2 value within the branch of the hysteresis curve between SN ($l_2 = -7.17$) and HB ($l_2 = -6.81$), there is a stable normal cycle (large amplitude LH) and a stable anovulatory cycle (small amplitude LH). A woman whose cycle is represented by one of these stable anovulatory cycles may be perturbed to a normal cycle by decreasing her l_2 parameter below -7.17, which effectively increases the stockpiling of her preantral follicles. However, additional stockpiling where l_2 becomes less than -7.54 results in irregular or chaotic cycling because of the period-doubling cascade. This observation suggests a curious biological hypothesis that a woman, who is anovulatory because of low LH, may benefit from additional preantral follicular mass but only up to a point where too much mass may lead to irregular cycling.

5. Bifurcation analysis for parameter κ

The parameter κ in (S1) modulates the effect of T on baseline LH synthesis via the term T^κ. Since the optimal parameter value $\kappa = 0.9176$ is positive but less than one, this synthesis rate increases with T and with κ but is slightly sublinear. If $\kappa > 1$ then this effect becomes more pronounced. P4 in the denominator of (S1) indicates inhibition of LH synthesis. An increase in κ reduces this inhibitory effect for a fixed level of P4. Here we examine the bifurcation diagram (Fig. 3) which plots maximum LH along a periodic or equilibrium solution against κ.

For values of κ less than 0.883, the only stable solution is an equilibrium (the light solid curve in the lower left of Fig. 3), which
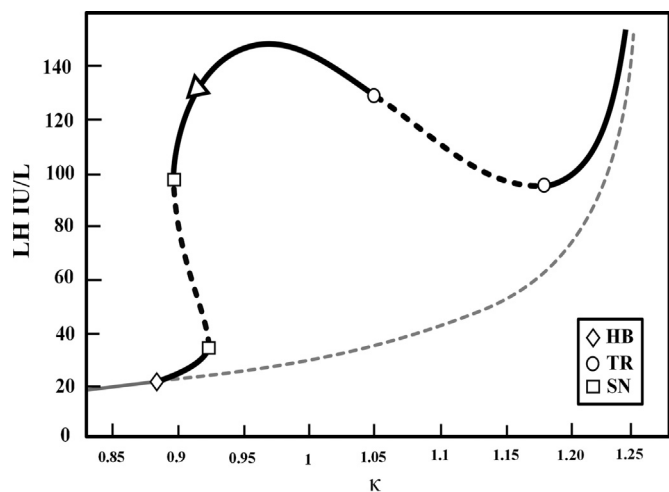
Fig. 3. Bifurcation diagram with respect to κ for (S1–S16) with remaining optimal parameters from Tables B1–B3. HB, SN and TR denote Hopf, saddle-node and torus bifurcations. The large $\triangle$ indicates the position of the cycle for the optimal value $\kappa=0.9176$. Heavy solid (dashed) curves denote stable (unstable) cycles. Light solid (dashed) curves denote stable (unstable) equilibria.
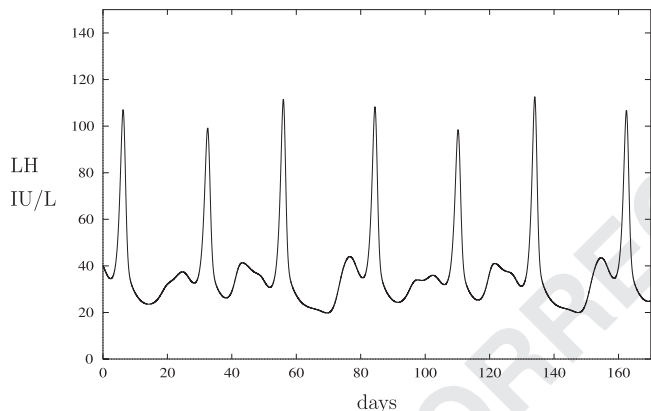

Fig. 4. LH model simulation for (S1–S16) when $\kappa=1.1$ is a solution residing on the invariant torus depicted in Fig. 3. The solution has a period of about 78 days as measured between the first and the fourth peaks and represents 3 menstrual cycles.
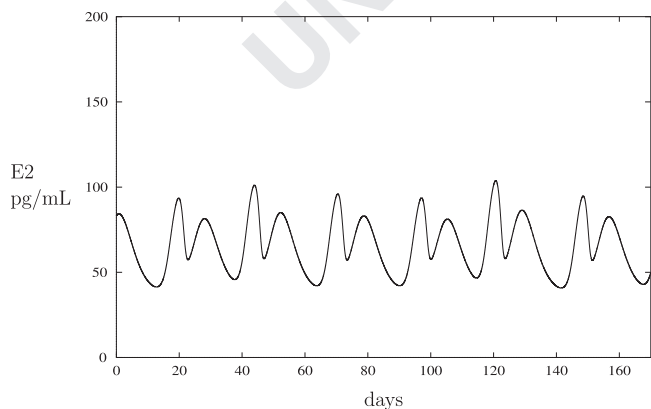

Fig. 5. E2 model simulation for (S1–S16) when $\kappa=1.1$ resides on the invariant torus. The low E2 levels indicate diminished dominant follicle development and anovulation.

represents an anovulatory cycle because the *LH* level is too low. At $\kappa=0.883$, a Hopf bifurcation (HB) occurs which results in a stable periodic solution (heavy solid curve) and an unstable equilibrium (light dashed curve that continues to the right from HB). This
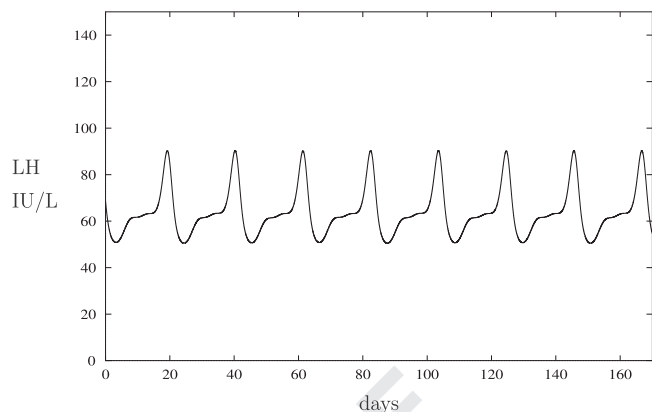

Fig. 6. LH model simulations when $\kappa=1.21$ has a period of 21 days and the cycle is anovulatory. LH levels range between 50 IU/L and 92 IU/L, which indicates a minimum LH much higher than normal.

anovulatory stable cycle exists until $\kappa=0.924$ where it coalesces with an unstable cycle and both disappear via a saddle-node (lower SN). The unstable cycle originates from a saddle-node (upper SN) at $\kappa=0.899$, which also produces the stable ovulatory cycle that continues to the normal cycle (large $\triangle$) at optimal $\kappa=0.9176$. The system maintains a stable periodic solution as κ increases to 1.065, where a torus bifurcation (TR) occurs. This bifurcation is a Naimark–Sacker bifurcation (Naimark, 1967; Sacker, 1964) of the return map of the periodic solution and this bifurcation destabilizes the periodic solution and surrounds it with an attracting invariant torus. Solutions on the torus approximate the periodic solution but, generally, may be periodic or irregular. Between the two TR's, i.e., for $1.065 < \kappa < 1.197$, the only attractor for system (S1–S16) is the invariant torus. For parameters just to the left of TR=1.065, the stable solution has a period of about 27 days and has an LH surge which is similar to the stable cycle (Fig. 1) for the optimal parameter set. For $\kappa=1.1$ (Fig. 4) just to the right of TR=1.065, the stable solution on the torus appears to have a period of approximately 78 days (measured between the first and fourth peaks) and represents three menstrual cycles of differing LH surge heights.

As κ increases from optimal value, the development of the dominant follicle is retarded as observed from a reduction in the amount of E2, which is proportional to follicular mass via (A1). Notice that if $\kappa=1.1$, the E2 levels only reach 100 pg/mL (Fig. 5 as compared to Fig. 1). Such a menstrual cycle will be anovulatory. At $\kappa=1.197$ the TR is a reverse torus bifurcation where the attracting torus shrinks to a periodic solution. This stable solution, which is plotted in Fig. 6 for $\kappa=1.21$, has a period of about 21 days and LH levels ranging between 50 IU/L and 92 IU/L but also is anovulatory because of insufficient development of the dominant follicle. Normal basal LH is less than 20 IU/L but the minimum LH for the anovulatory cycles in Figs. 4 and 6 is above that with the minimum LH in Fig. 6 about 50 IU/L. Hence, our model suggests that increased pituitary sensitivity to T results in anovulation indicated by high basal LH and lack of dominant follicle development.

6. Bifurcation analysis for parameters κ and t_3

Although many of the anovulatory cycles illustrated in Sections 3–5 exhibit similarities to PCOS cycles, none have high androgen levels characteristic of classical PCOS. In this section we show that increasing κ and increasing a model sensitive parameter in the auxiliary equation (A5) for testosterone result in cycles which are both anovulatory and hyperandrogenic. The parameter t_3 in (A5)
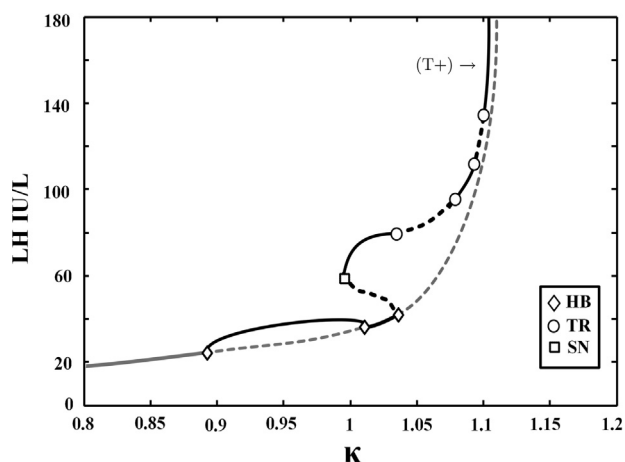
Fig. 7. Bifurcation diagram with respect to κ, with $t_3 = 1.5$. HB, SN an TR denote Hopf, saddle-node and torus bifurcations. Labeled point (T+) for elevated T designates location of solution corresponding to LH profiles in Fig. 8. Solid curves denote stable cycles or equilibria and dashed curves denote unstable cycles or equilibria.

represents the amount of T produced by small antral follicles (SmAn). Nestler et al. (1998) showed that isolated theca cells from PCOS women demonstrated an approximately four fold increase in insulin stimulated T biosynthesis when compared with theca cells from normally cycling women. Follicles harvested for their study ranged from between 4 mm and 12 mm in diameter, a range consistent with small antral and recruited follicle classifications (Gougeon, 1986).

Thus, to study how increasing the effects of T on the pituitary and on the ovaries alters cycle behavior, we consider bifurcation diagrams with respect to the pituitary T parameter κ (like Fig. 3) for increasing values of the ovarian T parameter t_3. Fig. 3 depicts maximum LH as κ varies for the optimal value $t_3 = 0.667$ in Table B3. As t_3 increases from $t_3 = 0.667$ to $t_3 = 1.5$ a sequence of bifurcations occurs which change the character of the κ bifurcation diagram (for details see Hendrix, 2013). Briefly, the lower branch of the hysteresis curve on the left in Fig. 3 touches the curve of equilibria at a degenerate Hopf point, i.e., a point where a Hopf bifurcation occurs because a complex pair of eigenvalues cross the imaginary axis with zero speed. As t_3 continues to increase, the degenerate Hopf point unfolds into two nondegenerate Hopf points. A similar unfolding of a degenerate Hopf bifurcation is described in Margolskee and Selgrade (2011), and an animation may be found at http://www4.ncsu.edu/selgrade/research.html.

The resulting bifurcation diagram when $t_3 = 1.5$ is shown in Fig. 7 and has four TR bifurcations. The stable upper branch of cycles at location (T+) in Fig. 7 exhibit significantly different serum hormone levels (see Fig. 8) compared to those when $t_3 = 0.667$. When $t_3 = 1.5$ and $\kappa = 1.1$ (see location (T+) in Fig. 7), LH and T levels are consistently elevated. E2 and P4 levels are suppressed reflecting a reduction in ovarian follicular activity. The elevation in circulating T is consistent with hyperandrogenic disorders. The follicular dynamics for this cycle are different from the normal cycle presented in Fig. 1.

In Fig. 9 we present the predictions for ovarian mass of preantral (PrA 1) and small antral (SmAn) follicular stages with a view of CL development (Lut1) for both the normal cycle (dashed curves) and the solution presented in Fig. 8 (solid curves). One can see that the mass of developing follicles for both stages is significantly elevated, a case which may manifest in the appearance of polycystic ovaries on ultrasound. The CL, in this case is diminished, suggesting the absence of ovulation. These predictions are the first we have seen through our investigations that reflect anovulatory and hyperandrogenic states simultaneously. These findings suggest multiple mechanisms may be implicated in disorders of this nature.

7. Summary and discussion

This model for hormonal regulation of the menstrual cycle includes the effects of the androgen testosterone on follicular development and on the synthesis of LH in the pituitary. The system of 16 differential equations contains stages of ovarian development which represent preantral and early antral follicles. Fitting the parameters to the data from Welt et al. (1999) and from Sinha-Hikim et al. (1998) produces simulations which accurately predict hormone levels of a normally cycling woman.

As with a simpler model (Harris-Clark et al., 2003), another stable periodic solution exists for the same parameter values but this cycle exhibits abnormal hormone levels and no LH surge. Hence, a woman represented by this model may cycle normally or abnormally based on initial hormone levels. If cycling is abnormal, it may be possible to adjust her hormone levels to perturb her cycle to a normal cycle. Numerical experiments indicate that the domain of attraction of the normal cycle is much larger than the domain of attraction of the abnormal cycle, i.e., it is much easier to pick initial conditions for a solution converging to the normal cycle. However, we do not have an estimate of the probability of convergence to the normal cycle. Here we do explain this bistability by the presence of hysteresis curves in bifurcation diagrams with respect to sensitive model parameters, m_2 (Fig. 2) and κ (Fig. 3).

Decreasing the follicular growth parameter m_2 prolongs the growth of the preantral follicular stage and results in a "stockpiling" of preantral follicles. In fact, continuing to decrease m_2 produces a cascade of period-doubling bifurcations resulting in chaotic menstrual cycle behavior (Hendrix et al., 2014) which we illustrate here using a bifurcation diagram drawn with the software XPPAUT (Ermentrout, 2002). Maciel et al. (2004) observed almost 5 times as many small preantral, gonadotropin-independent follicles in PCOS ovaries as compared to normal ovaries. A noninvasive method of counting these follicles would be useful to clinical endocrinologists for predicting reproductive abnormalities.

The parameter κ modulates the stimulatory effect of T on LH synthesis. Increasing κ causes basal LH levels to rise and the LH surge to be maintained (see Figs. 4 and 6) but suppresses follicular development to such an extent that ovulation cannot occur (see Fig. 5). Hence, increased pituitary sensitivity to T as a cause of anovulation is demonstrated by our model.

Anovulatory cycles which exhibit high androgen levels are characteristic of classical PCOS. This phenomenon is illustrated by increasing both the pituitary sensitivity to T (parameter κ) and the follicular production of T from small antral follicles (parameter t_3). Resulting simulations indicate anovulatory cycles with high levels of LH and T as well as reduced and acyclic E2 and P4 (Fig. 8). Thus, this model suggests that androgenic activity at the levels of both the pituitary and the ovaries may contribute to the etiology of PCOS.

Poretsky et al. (1999) suggests that insulin resistance (IR) is a characteristic of many PCOS women and results in hyperandrogenism. Specifically, IR causes increased insulin production to process glucose and increased insulin causes an increase in ovarian androgens. In the setting of our model, IR may be a reason for a higher than normal t_3 parameter value. Thus, a logical next step in unraveling the causes of PCOS will be to link a glucose-insulin model with our cycle regulation model with the ultimate goal of characterizing the interplay between glucoregulation and sexual endocrine control.
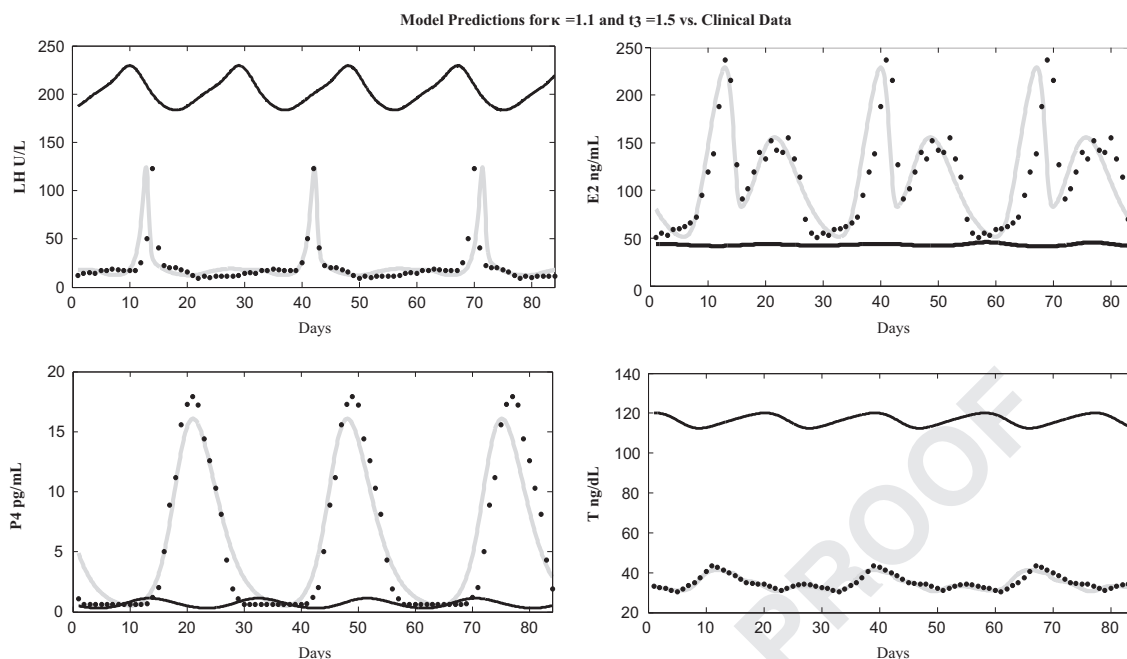
Fig. 8. Hormone predictions (dark curves) for $\kappa = 1.1$ with $t_3 = 1.5$ correspond to a solution at location (T+) as identified in Fig. 7. The high LH and T and the low E2 and P4 demonstrate the effects of increased sensitivity to T combined with elevated ovarian T production. The gray curves depict model simulations with optimal parameters approximating clinical data (Welt et al., 1999; Sinha-Hikim et al., 1998).
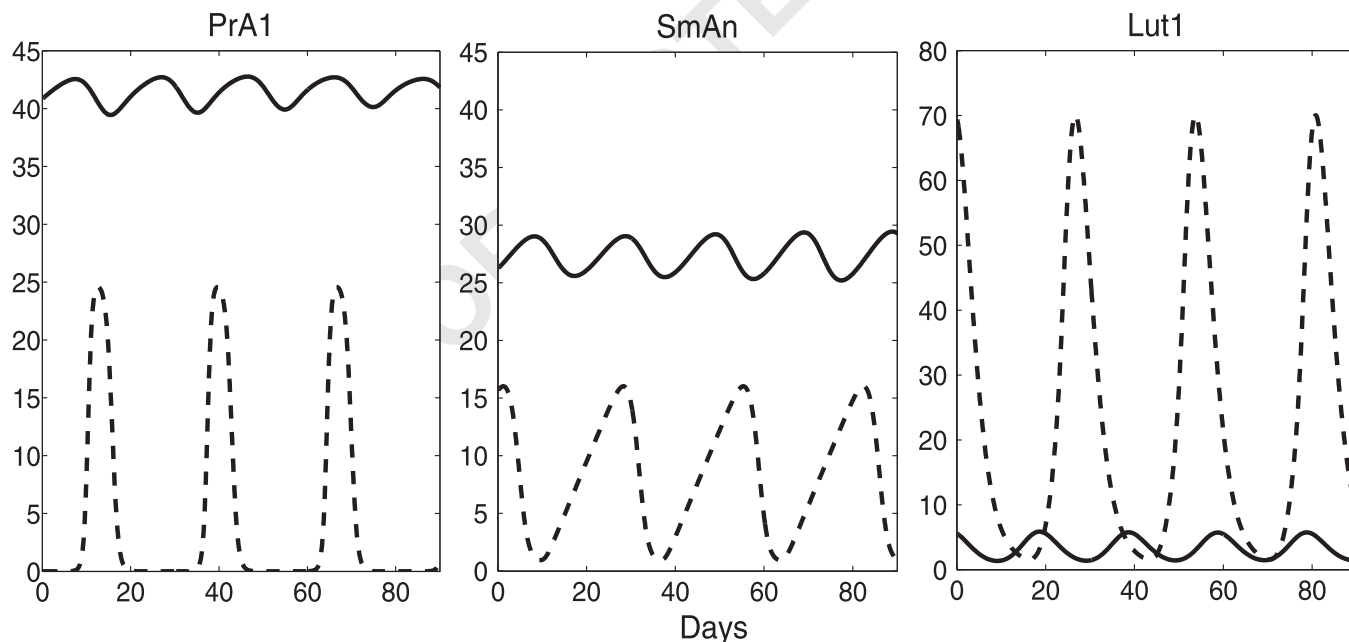

Fig. 9. Ovarian mass predictions for $\kappa = 1.1$ and $t_3 = 1.5$ (solid curves) compared with the normal solution (dashed curves) for parameters in Tables B1–B3. Demonstrated is the significant increase in preantral and small antral follicular mass and decrease in CL development versus the normal solution.

Appendix A. Differential equations and auxiliary equations

System of differential equations:

$$\frac{d}{dt}RP_{LH} = \frac{v_0 \cdot T(t-d_T)^\kappa + v_1 \cdot \dfrac{E2(t-d_E)^a}{(Km_{LH}^a + E2(t-d_E)^a)}}{(1 + P4(t-d_P)/Ki_{LH})}$$

$$- k_{LH} \cdot \frac{(1 + c_{LHp} \cdot P4^\delta)}{(1 + c_{LHe} \cdot E2)} \cdot RP_{LH} \qquad (S1)$$

$$\frac{d}{dt}LH = \frac{1}{v} \cdot k_{LH} \cdot \frac{(1 + c_{LHp} \cdot P4^\delta)}{(1 + c_{LHe} \cdot E2)} \cdot RP_{LH} - r_{LH} \cdot LH \qquad (S2)$$

$$\frac{d}{dt}RP_{FSH} = \frac{V_{FSH}}{1 + \left(\dfrac{InhA(t-d_{InhA})}{Ki_{FSHa}}\right) + \left(\dfrac{InhB(t-d_{InhB})}{Ki_{FSHb}}\right)}$$

$$- k_{FSH} \cdot \frac{(1 + c_{FSHp} \cdot P4)}{(1 + c_{FSHe} \cdot E2^\zeta)} \cdot RP_{FSH} \qquad (S3)$$

$$\frac{d}{dt}FSH = \frac{1}{v} \cdot k_{FSH} \cdot \frac{(1 + c_{FSHp} \cdot P4)}{(1 + c_{FSHe} \cdot E2^\zeta)} \cdot RP_{FSH} - r_{FSH} \cdot FSH \qquad (S4)$$

$$\frac{d}{dt}PrA1 = m_1 - m_2 \cdot T^\eta \cdot PrA1 \cdot PrA2 \qquad (S5)$$

$$\frac{d}{dt}PrA2 = m_2 \cdot T^\eta \cdot PrA1 \cdot PrA2 - m_3 \cdot \frac{FSH^\nu}{Km_{FSH}^\nu + FSH^\nu} \cdot PrA2 \cdot SmAn \tag{S6}$$

$$\frac{d}{dt}SmAn = m_3 \cdot \frac{FSH^\nu}{Km_{FSH}^\nu + FSH^\nu} \cdot PrA2 \cdot SmAn$$
$$- b \cdot FSH^\varrho \cdot SmAn \cdot RcF \tag{S7}$$

$$\frac{d}{dt}RcF = b \cdot FSH^\varrho \cdot SmAn \cdot RcF + (c_1 \cdot FSH - c_2 \cdot LH^\alpha) \cdot RcF \tag{S8}$$

$$\frac{d}{dt}DmF = c_2 \cdot LH^\alpha \cdot RcF + (c_3 \cdot LH^\beta - c_4 \cdot LH^\xi) \cdot DmF \tag{S9}$$

$$\frac{d}{dt}OvF = c_4 \cdot LH^\xi \cdot DmF - c_5 \cdot LH^\gamma \cdot OvF \tag{S10}$$

$$\frac{d}{dt}CL1 = c_5 \cdot LH^\gamma \cdot OvF - d_1 \cdot CL1 \tag{S11}$$

$$\frac{d}{dt}CL2 = d_1 \cdot CL1 - d_2 \cdot CL2 \tag{S12}$$

$$\frac{d}{dt}Lut1 = d_2 \cdot CL2 - k_1 \cdot Lut1 \tag{S13}$$

$$\frac{d}{dt}Lut2 = k_1 \cdot Lut1 - k_2 \cdot Lut2 \tag{S14}$$

$$\frac{d}{dt}Lut3 = k_2 \cdot Lut2 - k_3 \cdot Lut3 \tag{S15}$$

$$\frac{d}{dt}Lut4 = k_3 \cdot Lut3 - k_4 \cdot Lut4 \tag{S16}$$

Auxiliary equations:

$$E2 = e_0 + e_1 \cdot DmF + e_2 \cdot Lut4 \tag{A1}$$

$$P4 = p_1 \cdot Lut3 + p_2 \cdot Lut4 \tag{A2}$$

$$InhA = h_0 + h_1 \cdot OvF + h_2 \cdot Lut2 + h_3 \cdot Lut3 \tag{A3}$$

$$InhB = j_1 + j_2 \cdot PrA2 + j_3 \cdot SmAn + j_4 \cdot RcF + j_5 \cdot OvF^2 + j_6 \cdot Lut1 \tag{A4}$$

$$T = t_1 + t_2 \cdot PrA2 + t_3 \cdot SmAn + t_4 \cdot RcF + t_5 \cdot DmF$$
$$+ t_6 \cdot OvF + t_7 \cdot CL1 + t_8 \cdot Lut1 + t_9 \cdot Lut3 \tag{A5}$$

Appendix B. Parameter tables and initial conditions

Initial conditions for normal and abnormal cycles as plotted in Fig. 1 are given in Table B4.

Table B1
Parameters for pituitary equations (S1–S4) optimized using the data of Welt et al. (1999).

Parameter	Value	Unit
v_0	39.75	dL · IU/ng · day
κ	0.91761	dimensionless
v_1	153.66	IU/day
a	7.3964	dimensionless
Ki_{LH}	13.6395	ng/mL
Km_{LH}	52.0665	pg/mL
k_{LH}	18	1/day
c_{LHp}	0.98236	mL/ng
c_{LHe}	0.80821	mL/pg
δ	2	dimensionless
r_{LH}	14	1/day

Table B1 (continued)

Parameter	Value	Unit
v_{FSH}	287.269	IU/day
Ki_{FSHa}	6.3	IU/mL
Ki_{FSHb}	3000	pg/mL
k_{FSH}	3.86281	1/day
c_{FSHp}	1.261	mL/ng
c_{FSHe}	0.00025	mL/pg
ζ	2	dimensionless
r_{FSH}	8.21	1/day
ν	2.5	L

Table B2
Parameters for ovarian equations (S5–S16) optimized using the data of Welt et al. (1999) and Sinha-Hikim et al. (1998).

Parameter	Value	Unit
α	0.69	dimensionless
β	0.693	dimensionless
γ	0.002	dimensionless
η	1.1617	dimensionless
ν	8	dimensionless
ϱ	0.45	dimensionless
ξ	0.952	dimensionless
b	0.017	L/day
c_1	0.087	L/μg
c_2	0.115	1/day
c_3	0.0534	1/day
c_4	0.0369	1/day
c_5	0.482	1/day
d_1	0.706	1/day
d_2	0.6515	1/day
k_1	0.695	1/day
k_2	0.872	1/day
k_3	1.039	1/day
k_4	1.052	1/day
m_1	0.927	1/day
m_2	0.000868	1/day
m_3	0.09	1/day
Km_{FSH}	6.53	1/day

Table B3
Parameters for auxiliary equations (A1–A5) optimized using the data of Welt et al. (1999) and Sinha-Hikim et al. (1998).

Parameter	Value	Unit
e_0	37.4	ng/L
e_1	2.3	1/kL
e_2	2.724	1/kL
h_0	0.0525	IU/L
h_1	0.0251	IU/L/μg
h_2	0.06315	IU/L/μg
h_3	0.16	IU/L/μg
p_1	0.2548	1/L
p_2	0.133	1/L
j_1	0.001	pg/L
j_2	1.72	1/L
j_3	5.03	1/L
j_4	4.32	1/L
j_5	0.0012	1/L
j_6	0.001	1/L
t_1	13.1354	ng/dL
t_2	0.704	1/dL
t_3	0.667	1/dL
t_4	0.7436	1/dL
t_5	0	1/dL
t_6	0.097	1/dL
t_7	0	1/dL
t_8	0.21	1/dL
t_9	0.0932	1/dL

Table B4

Initial conditions for normal and abnormal cycles as plotted in Fig. 1.

Variable	Normal	Abnormal
RP_{LH}	396	268
LH	22.0	23.1
RP_{FSH}	30.2	39.7
FSH	11.2	9.0
$PrA1$	2.3	12.4
$PrA2$	0.42	0.4
$SmAn$	24.4	0.57
RcF	0.21	5.62
DmF	0.697	28.0
OvF	1.55	42.0
$CL1$	1.46	26.6
$CL2$	2.38	25.2
$Lut1$	3.48	20.3
$Lut2$	4.03	14.4
$Lut3$	4.64	11.0
$Lut4$	6.27	10.0

References

Alvarez-Blasco, F., Botella-Carretero, J.I., San Millan, J.L., et al., 2006. Prevalence and characteristics of the polycystic ovary syndrome in overweight and obese women. Arch. Intern. Med. 166, 2081–2086.

Azziz, R., Woods, K.S., Reyna, R., Key, T.J., Knochenhauer, E.S., Yildiz, B.O., 2004. The prevalence and features of the polycystic ovary syndrome in an unselected population. J. Clin. Endocrinol. Metab. 89 (6), 2745–2749. http://dx.doi.org/10.1210/jc.2003-032046 ⟨http://jcem.endojournals.org/cgi/content/abstract/89/6/2745⟩.

Azziz, R., Carmina, E., Dewailly, D., Diamanti-Kandarakis, E., Escobar-Morreale, H.F., Futterweit, W., et al., 2009. The androgen excess and PCOS Society criteria for the polycystic ovary syndrome: the complete task force report. Fertil. Steril. 91 (2), 456–488 ⟨http://www.sciencedirect.com/science/article/B6T6K-4TRR8Y5-1/2/⟩.

Baird, R.T., Horton, R., Longcope, C., Tait, J.F., 1969. Steroid dynamics under steady-state conditions. Recent Prog. Hormon. Res. 25, 611–664.

Blank, S.K., McCartney, C.R., Marshall, J.C., 2006. The origins and sequelae of abnormal neuroendocrine function in polycystic ovary syndrome. Hum. Reprod. Update 12 (4), 351–361. http://dx.doi.org/10.1093/humupd/dml017 ⟨http://humupd.oxfordjournals.org/content/12/4/351.abstract⟩.

Bogumil, R.J., Ferin, M., Rootenberg, J., Speroff, L., Vande Wiele, R.L., 1972. Mathematical studies of the human menstrual cycle. I. Formulation of a mathematical model. J. Clin. Endocrinol. Metab. 35 (1), 126–143 ⟨http://www.ncbi.nlm.nih.gov/pubmed/5064156⟩.

Bogumil, R.J., Ferin, M., Wiele, R.L.V., 1972. Mathematical studies of the human menstrual cycle. II. Simulation performance of a model of the human menstrual cycle. J. Clin. Endocrinol. Metab. 35 (1), 144–156. http://dx.doi.org/10.1210/jcem-35-1-144 ⟨http://jcem.endojournals.org/cgi/content/abstract/35/1/144⟩.

Chen, C., Ward, J., 2014. A mathematical model for the human menstrual cycle. Math. Med. Biol. 31, 65–86. http://dx.doi.org/10.1093/imammb/dqs048.

De Leo, V., Morgante, G., 1998. Hormonal effects of flutamide in young women with polycystic ovary syndrome. J. Clin. Endocrinol. Metab. 83 (1), 99–102.

Eagleson, C.A., Gingrich, M.B., Pastor, C.L., Arora, T.K., Burt, C.M., Evans, W.S., et al., 2000. Polycystic ovarian syndrome: evidence that flutamide restores sensitivity of the gonadotropin-releasing hormone pulse generator to inhibition by estradiol and progesterone. J. Clin. Endocrinol. Metab. 85 (11), 4047–4052. http://dx.doi.org/10.1210/jc.85.11.4047 ⟨http://jcem.endojournals.org/content/85/11/4047.abstract⟩.

Ermentrout, B., 2002. Simulating, Analyzing and Animating Dynamical Systems. SIAM, Philadelphia.

Franks, S., Stark, J., Hardy, K., 2008. Follicle dynamics and anovulation in polycystic ovary syndrome. Hum. Reprod. Update 14 (4), 1–12 ⟨http://humupd.oxfordjournals.org/content/early/2008/05/22/⟩.

Gougeon, A., 1986. Dynamics of follicular growth in the human: a model from preliminary results. Hum. Reprod. (Oxford, England) 1 (2), 81–87 ⟨http://www.ncbi.nlm.nih.gov/pubmed/3558758⟩.

Harris-Clark, L., Schlosser, P.M., Selgrade, J.F., 2003. Multiple stable periodic solutions in a model for hormonal control of the menstrual cycle. Bull. Math. Biol. 65 (1), 157–173. http://dx.doi.org/10.1006/bulm.2002.0326 ⟨http://www.ncbi.nlm.nih.gov/pubmed/12597121⟩.

Hendrix, A.O., 2013. Modeling the effects of androgens on hormonal regulation of the menstrual cycle. (Ph.D. thesis), North Carolina State University. ⟨http://www.lib.ncsu.edu/resolver/1840.16/9085⟩.

Hendrix, A.O., Hughes, C.L., Selgrade, J.F., 2014. Modeling endocrine control of the pituitary-ovarian axis: androgenic influence and chaotic dynamics. Bull. Math. Biol. 76, 136–156.

Hotchkiss, J., Knobil, E., 1994. The menstrual cycle and its neuroendocrine control. In: Knobil, E., Neill, J. (Eds.), The Physiology of Reproduction, Second Edition Raven Press, New York, pp. 711–750.

Karch, F., Dierschke, D., Weick, R., Yamaji, T., Hotchkiss, J., Knobil, E., 1973. Positive and negative feedback control by estrogen of luteinizing hormone secretion in the rhesus monkey. Endocrinology 92 (3), 799–804. http://dx.doi.org/10.1210/endo-92-3-799 ⟨http://endo.endojournals.org/cgi/content/abstract/92/3/799⟩.

Keener, J., Sneyd, J., 2009. Mathematical Physiology I: Cellular Physiology, second ed. Springer-Verlag, New York.

Liu, J.H., Yen, S.S.C., 1983. Induction of midcycle surge by ovarian steriods in women: a critical evaluation. J. Clin. Endocrinol. Metab. 57 (4), 797–802.

Maciel, G.A.R., Baracat, E.C., Benda, J.A., Markham, S.M., Hensinger, K., Chang, R.J., et al., 2004. Stockpiling of transitional and classic primary follicles in ovaries of women with polycystic ovary syndrome. J. Clin. Endocrinol. Metab. 89 (11), 5321–5327. http://dx.doi.org/10.1210/jc.2004-0643 ⟨http://www.ncbi.nlm.nih.gov/pubmed/15531477⟩.

Margolskee, A., Selgrade, J.F., 2011. Dynamics and bifurcation of a model for hormonal control of the menstrual cycle with inhibin delay. Math. Biosci. 234, 95–107. http://dx.doi.org/10.1016/j.mbs.2011.09.001.

Margolskee, A., Selgrade, J.F., 2013. A lifelong model for the female reproductive cycle with an antimüllerian hormone treatment to delay menopause. J. Theor. Biol. 326 (0), 21–35. http://dx.doi.org/10.1016/j.jtbi.2013.02.007 ⟨http://www.sciencedirect.com/science/article/pii/S0022519313000751⟩.

Melrose, P., Gross, L., 1987. Steroid effects on the secretory modalities of gonadotropin-releasing hormone release. Endocrinology 121 (1), 190–199. http://dx.doi.org/10.1210/endo-121-1-190 ⟨http://endo.endojournals.org/content/121/1/190.abstract⟩.

Naimark, J., 1967. Motions close to doubly asymptotic motions. Sov. Math. Dokl. 8, 231–611.

Nelder, J., Mead, R., 1965. A simplex method for function minimization. Comput. J. 7, 308–313.

Nestler, J., Jakubowicz, D., de Vargas, A., Brink, C., Quintero, N., Medina, F., 1998. Insulin stimulates testosterone biosynthesis by human thecal cells from women with polycystic ovary syndrome by activating its own receptor and using inositolglycan mediators as the signal transduction system. J. Clin. Endocrinol. Metab. 83, 2001–2005.

Ojeda, S.R., 2012. Female reproductive function. In: Kovacks, W.J., Ojeda, S.R. (Eds.), Textbook of Endocrine Physiology, sixth ed. New York, pp. 228–238. ISBN: 978-0-19-974412-1 (chapter 8).

Pasteur, R., 2008. A Multiple-Inhibin Model for the Human Menstrual Cycle. Ph.D. thesis; North Carolina State University. ⟨http://www.lib.ncsu.edu/resolver/1840.16/5587⟩.

Pielecka, J., Quaynor, S.D., Moenter, S.M., 2006. Androgens increase gonadotropin-releasing hormone neuron firing activity in females and interfere with progesterone negative feedback. Endocrinology 147 (3), 1474–1479. http://dx.doi.org/10.1210/en.2005-1029 ⟨http://www.ncbi.nlm.nih.gov/pubmed/16339200⟩.

Plouffe, L.J., Luxenberg, S.N., 1992. Biological modeling on a microcomputer using standard spreadsheet and equation solver programs: the hypothalamic-pituitary-ovarian axis as an example. Comput. Biomed. Res. 25 (2), 117–130. http://dx.doi.org/10.1016/0010-4809(92)90015-3 ⟨http://www.sciencedirect.com/science/article/pii/0010480992900153⟩.

Poretsky, L., Cataldo, N., Rosenwaks, Z., Giudice, L., 1999. The insulin-related ovarian regulatory system in health and disease. Endocr. Rev. 20, 535–582.

Reinecke, I., Deuflhard, P., 2007. A complex mathematical model of the human menstrual cycle. J. Theor. Biol. 247 (2), 303–330. http://dx.doi.org/10.1016/j.jtbi.2007.03.011 ⟨http://www.ncbi.nlm.nih.gov/pubmed/17448501⟩.

Röblitz, S., Stötzel, C., Deuflhard, P., Jones, H., Azulay, D.O., van der Graaf, P., et al., 2013. A mathematical model of the human menstrual cycle for the administration of GnRH analogues. J. Theor. Biol. 321, 8–27. http://dx.doi.org/10.1016/j.jtbi.2012.11.020.

Sacker, R.J., 1964. On Invariant Surfaces and Bifurcation of Periodic Solutions of Ordinary Differential Equations (Ph.D. thesis), New York University, IMM-NYU.

Sar, M., Lubahn, D.B., French, F.S., Wilson, E.M., 1990. Immunohistochemical localization of the androgen receptor in rat and human tissues. Endocrinology 127 (6), 3180–3186. http://dx.doi.org/10.1210/endo-127-6-3180 ⟨http://endo.endojournals.org/content/127/6/3180.abstract⟩.

Schlosser, P., Selgrade, J., 2000. A model of gonadotropin regulation during the menstrual cycle in women: qualitative features. Environ. Health Perspect. 108 (5), 873–881.

Selgrade, J.F., Harris, L.A., Pasteur, R.D., 2009. A model for hormonal control of the menstrual cycle: structural consistency but sensitivity with regard to data. J. Theor. Biol. 260 (4), 572–580. http://dx.doi.org/10.1016/j.jtbi.2009.06.017 ⟨http://dx.doi.org/10.1016/j.jtbi.2009.06.017⟩.

Sinha-Hikim, I., Arver, S., Beall, G., Shen, R., Guerrero, M., Sattler, F., et al., 1998. The use of a sensitive equilibrium dialysis method for the measurement of free testosterone levels in healthy, cycling women and in human immunodeficiency virus-infected women. J. Clin. Endocrinol. Metab. 83 (4), 1312–1318 ⟨http://www.ncbi.nlm.nih.gov/pubmed/9543161⟩.

Takeda, H., Chodak, G., Mutchnik, S., Nakamoto, T., Chang, C., 1990. Immunohistochemical localization of androgen receptors with mono- and polyclonal antibodies to androgen receptor. J. Endocrinol. 126 (1), http://dx.doi.org/10.1677/joe.0.1260017 17–NP. ⟨http://joe.endocrinology-journals.org/content/126/1/17.abstract⟩.

Wang, C.F., Lasley, B.L., Lein, A., Yen, S.S.C., 1976. The functional changes of the pituitary gonadotrophs during the menstrual cycle. J. Clin. Endocrinol. Metab. 42 (4), 718–728. http://dx.doi.org/10.1210/jcem-42-4-718 ⟨http://jcem.endojournals.org/content/42/4/718.abstract⟩.

Welt, C.K., McNicholl, D.J., Taylor, A.E., Hall, J.E., 1999. Female reproductive aging is marked by decreased secretion of dimeric inhibin. J. Clin. Endocrinol. Metab. 84 (1), 105–111 ⟨http://www.ncbi.nlm.nih.gov/pubmed/9920069⟩.

Wright, M., 1996. Direct search methods: once scorned now respectable. In: Griffiths, D., Watson, G. (Eds.), Numerical Analysis 1995. Proceedings of the 1995 Dundee Biennial Conference in Numerical Analysis. Pitman Research Notes in Mathematics. Addison Wesley Longman, London, pp. 191–208.

Yasin, M., Dalkin, A., Haisenleder, D.J., Marshal, C.J., 1996. Testosterone is required for gonadotropin-releasing hormone stimulation of luteinizing hormone – P messenger ribonucleic acid expression in female rats. Endocrinology 137 (4), 1265–1271.

Yen, S.S.C., 1999a. Polycystic ovarian syndrome hyperandrogenic chronic anovulation. In: Yen, S.S.C., Jaffe, R.B., Barbieri, R.L. (Eds.), Reproductive Endocrinology, Physiology, Pathophysiology and Clinical Management, Fourth Edition W.B. Sauders Co, Philadelphia, pp. 436–478.

Yen, S.S.C., 1999b. The human menstrual cycle: neuroendocrine regulation. In: Yen, S.S.C., Jaffe, R.B., Barbieri, R.L. (Eds.), Reproductive Endocrinology. Physiology, Pathophysiology and Clinical Management, Fourth ed. W.B. Saunders Co., Philadelphia, pp. 191–217.

Zeeman, M., Gokhman, D., Weckesser, W., 2003. Resonance in the menstrual cycle: a new model of the LH surge. Reprod. Biomed. Online 7, 295–300.

Zeleznik, A.J., Benyo, D.F., Hotchkiss, J., Knobil, E., 1994. Control of follicular development, corpus luteum function, and the recognition of pregnancy in higher primates. In: Knobil, E., Neill, J. (Eds.), The Physiology of Reproduction, Second Edition Raven Press, pp. 751–782.